Vol. 50 (2019) *Acta Physica Polonica B* No 3

# ON THE $X(17)$ LIGHT-PARTICLE CANDIDATE OBSERVED IN NUCLEAR TRANSITIONS*

A.J. Krasznahorkay, M. Csatlós, L. Csige, D. Firak, J. Gulyás
Á. Nagy, N. Sas, J. Timár, T.G. Tornyi

Institute for Nuclear Research, Hungarian Academy of Sciences (MTA Atomki)
P.O. Box 51, 4001 Debrecen, Hungary

A. Krasznahorkay

CERN, Geneva, Switzerland

*(Received November 21, 2018)*

Recently, we observed an anomalous internal pair creation for the M1 transition depopulating the 18.15 MeV isoscalar $1^+$ state in $^8$Be. The deviation from the theoretical prediction can be described by assuming the creation and subsequent decay of a new, light boson with a mass of 16.7 MeV/$c^2$. In order to clarify the interpretation, we re-investigated the $^8$Be anomaly with an improved and independent setup. We have confirmed the signal of the assumed $X(17)$ particle and constrained its mass ($m_0c^2 =$ 17.01(16) MeV) and branching ratio compared to the $\gamma$-decay ($B_x = 6(1) \times 10^{-6}$). We investigated also the high-energy (21 MeV) $J^\pi = 0^- \to 0^+$ transition in $^4$He and got a consistent result for the $X(17)$ particle.

DOI:10.5506/APhysPolB.50.675

## 1. Introduction

Recently, we measured electron–positron angular correlations for the 17.6 MeV, and 18.15 MeV, $J^\pi = 1^+ \to J^\pi = 0^+$ M1 transitions in $^8$Be and anomalous angular correlation, a significant peak-like enhancement relative to the internal pair creation was observed at large angles in the angular correlation of the 18.15 MeV transition [1]. This was interpreted as the creation and decay of an intermediate particle $X(17)$ with a mass of $m_0c^2 = 16.70 \pm 0.35(\text{stat.}) \pm 0.5(\text{syst.})$ MeV.

* Presented at the Zakopane Conference on Nuclear Physics "Extremes of the Nuclear Landscape", Zakopane, Poland, August 26–September 2, 2018.

The possible relation of the $X(17)$ boson to the dark matter problem and the fact that it might explain the $(g-2)_\mu$ puzzle, triggered high theoretical and experimental interest in the particle and hadron physics community [2].

Zhang and Miller discussed in detail if nuclear physics could explain the anomaly observed in the internal pair production in the $^8$Be nucleus, however they could not describe it within nuclear physics [3].

Our observation was explained by Feng *et al.* [4, 5] by introducing a 16.7 MeV, $J^\pi = 1^+$ vector gauge boson $X(17)$, which may mediate a fifth force with some coupling to SM particles. Thus, the $X(17)$ boson could be produced in the decay of an excited state to the ground state, $^8\mathrm{Be}^* \to {}^8\mathrm{Be} + X(17)$, followed by a decay through $X(17) \to e^+e^-$. At the same time Ellwanger and Moretti made another possible interpretation [6] of our experimental results assuming a light, pseudoscalar particle. Given the quantum-numbers of the $^8\mathrm{Be}^*$ and $^8$Be states, the $X(17)$ boson can indeed be a $J^\pi = 0^-$ pseudoscalar particle, if it is emitted with an $L = 1$ orbital momentum.

In the present work, we re-investigated the $^8$Be anomaly with an improved and independent setup, and studied also $e^+e^-$ pair correlations in a high-energy $0^- \to 0^+$ transition of $^4$He.

## 2. Experiments

To populate the 17.6 and 18.15 MeV $1^+$ excited states in $^8$Be selectively, we used the $^7\mathrm{Li}(p,\gamma)^8\mathrm{Be}$ reaction at the $\mathrm{E}_p = 441$ keV and the $E_p = 1030$ keV resonances [7]. The experiment was performed at the new 2-MV Tandetron accelerator at the MTA Atomki. A proton beam with a typical current of 1.0 $\mu$A impinged on 15 $\mu$g/cm$^2$ LiF (used at the $\mathrm{E}_p = 441$ keV resonance) and 300 $\mu$g/cm$^2$ thick Li target evaporated on 20 $\mu$g/cm$^2$ thick carbon foils (used at the $E_p = 1030$ keV resonance). The average energy loss of the protons in the targets was 9 keV and 70 keV, so the actual proton energy was 450 and 1100 keV. In contrast to our previous experiment [1, 8], we used a much thinner $^{12}$C backing and we increased the number of telescopes (from 5 to 6), which resulted in a different pair detection efficiency as a function of the correlation angle. As a considerable improvement, we replaced the gas-filled MWPC detectors with a double-sided silicon strip detector (DSSSD) array.

The $e^+e^-$ pairs were detected by six plastic scintillator + DSSSD detector telescopes placed in a plain perpendicular to the beam direction. Their relative angles were 0°, 60°, 120°, 180° 240° and 300°. The size of the scintillators was $82 \times 86 \times 80$ mm$^3$. The positions of the hits were registered by the DSSSD detectors having strip widths of 3 mm. The telescope detectors were placed around the vacuum chamber made of a carbon fibre tube with a wall thickness of 1 mm.

$\gamma$ rays were also detected for monitoring purposes. A $\epsilon_{\rm rel} = 100\%$ HPGe detector was used at 25 cm from the target to detect the 18.15 MeV $\gamma$ rays produced in the $^7$Li$(p,\gamma)^8$Be reaction.

In order to populate the wide ($\Gamma = 0.84$ MeV) $0^-$ second excited state ($E_x = 21.1$ MeV) in $^4$He [9], we used the $^3$H$(p,\gamma)^4$He reaction at $E_p =$ 1.000 MeV bombarding energy, which is just below the threshold of the $(p,n)$ reaction ($E_{\rm thr} = 1.018$ MeV). The energy accuracy of the Tandetron accelerator was better than 1 keV. This state overlaps with the first excited state in $^4$He ($J^\pi = 0^+$, $E_x = 20.21$ MeV, $\Gamma = 0.50$ MeV), which was also excited at the same time and deexcited by an E0 transition.

The target used for the measurements was a tritiated titanium disk with a thickness of 3.0 mg/cm$^2$ evaporated previously on a 0.4 mm thick Mo disk. The concentration of the tritium atoms was $2.66 \times 10^{20}$ atoms/cm$^2$. The disk was cooled down to liquid $N_2$ temperature to prevent the evaporation of $^3$H.

## 3. Efficiency calibration of the $e^+e^-$ spectrometer

The well-known, strong 6.05-MeV IPC transition ($0^+ \to 0^+$, E0) following the $^{19}$F$(p,\alpha\, e^+e^-)^{16}$O reaction was applied to perform the energy calibration of the spectrometer.

The pair correlation efficiency of the telescopes was calibrated by using the same dataset but with uncorrelated $e^+e^-$ pairs of consecutive events. Accordingly, an energy-independent approximation of the efficiency curve could be extracted.

Such an approximation is accurate when only the central volume of the telescopes is in use. This condition was automatically fulfilled in our previous experiments, when MWPC detectors were used with an effective area of $30 \times 30$ mm$^2$.

However, the size of the DSSSD detectors used in the present experiment is $50 \times 50$ mm$^2$ resulting in a high probability of event loss when one of the particles escapes from the scintillator. It results in an efficiency reduction near the surface of the scintillator causing minor deviations in the efficiency curve. Thus, the energy dependence of the efficiency calibration was simulated by the Geant3 code (for the same $e^+e^-$ sum-energy gate as we used in the experimental data reduction) and taken into account as a correction for the experimentally determined efficiency curve.

The efficiency curve differs considerably for the present and previous setups, therefore, the present results could be considered as an independent measurement in the sense that any geometry-related systematic effect is eliminated from the measured data.

## 4. Subtraction of the background caused by cosmic rays

Figure 1 shows a $\gamma$-ray spectrum measured in the $^7$Li$(p,\gamma)^8$Be reaction at the $E_p = 441$ keV resonance. We can nicely see the 17.64 MeV transition going to the ground state of $^8$Be and a 14.61 MeV transition to the broad first excited state, but no background transitions from 8 to 18 MeV. This was expected, as the reaction has an exceptionally large $Q$-value of 17.25 MeV [7].

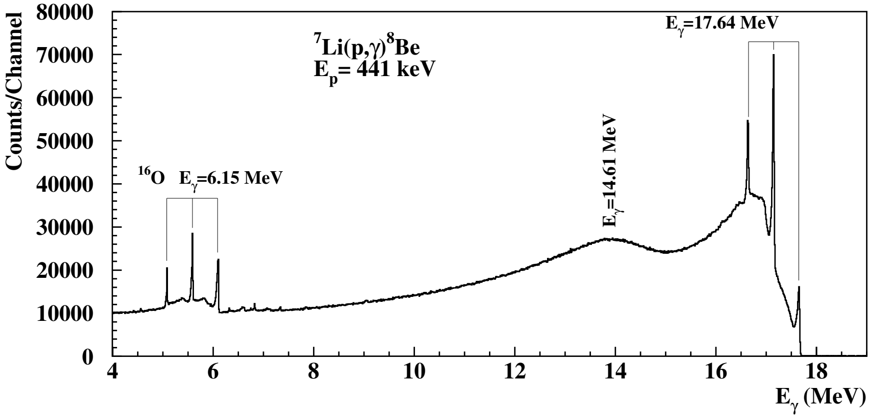


Fig. 1. A typical $\gamma$-ray spectrum measured at the $E_p = 441$ keV resonance.

However, in the $e^+e^-$ spectrometer, the cosmic ray background had to be taken into account. The background was measured for two weeks, before and after the experiment, and was subtracted with an experimentally determined factor from the results by using the same gates and conditions as for the in-beam data. The subtraction factor was derived by setting a high-energy gate ($E$(sum) = 25–50 MeV) on the cosmic rays for both cases (in-beam and off-beam). The cosmic ray background subtraction was then performed until eliminating all events within the high-energy gate.

The shape of the cosmic-ray background angular correlations determined for the 18 MeV gate is found to be completely different for the 5 detector and 6 detector configurations.

In order to get a reduction of the cosmic-ray background, an active shield was installed above the $e^+e^-$ spectrometer, which was constructed from 13 units of 1.0 cm thick, 4.5 cm wide and 100 cm long plastic scintillators. Half of the yield of the cosmic rays could be suppressed this way.

## 5. Results for the $^8$Be transitions

Figure 2 shows our experimental results for the sum energy spectrum of coincidence events (a), and the angular correlation (b) of $e^+e^-$ pairs measured at the proton absorption resonance at $E_p = 441$ keV. In order to check the efficiency of the experimental setup, we used the angular correlation determined for the 6.05 MeV E0 transition following the $^{19}\mathrm{F}(p,\alpha)^{16}\mathrm{O}$ reaction. It is shown in the upper curve of Fig. 2 (b) together with the simulated results for an E0 transition.

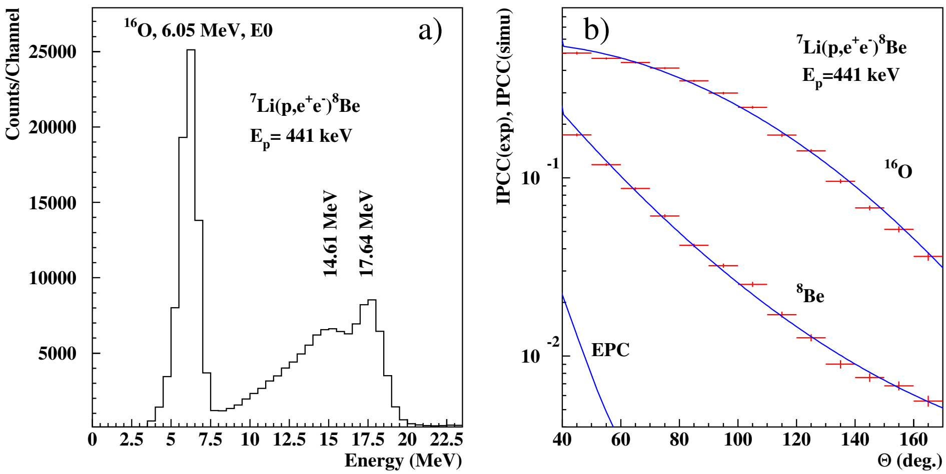


Fig. 2. (Color online) Measured sum energy spectrum (a) and angular correlation (b) of the $e^+e^-$ pairs originated from the decay of the 17.6 MeV resonance compared with the simulated angular correlations [8] assuming M1+1.0%E1 mixed transitions (solid blue curve). The contribution of external pair creation in the simulations caused by the 17.6 MeV $\gamma$ rays is shown at the bottom of the figure marked by EPC.

A typical $\gamma$-spectrum measured at $E_p = 1100$ keV is shown in Fig. 3 (a). The 18.15 MeV ($1^+ \to 0^+$ g.s.) photopeak and its single and double escape peaks are clearly visible. The broad peak at 15.15 MeV corresponds to the 15.15 MeV ($1^+ \to 2^+$ 3.03 MeV) transition.

The energy resolution of the peaks reflects both the width of the resonance ($\Gamma = 168$ keV) and the energy loss in the target. The branching ratio of the $\gamma$ transition from the 18.15 MeV $1^+$ state to the ground state and to the $2^+$ state is 30% and 70%, respectively [7]. The transition to the ground state from this state is much less favored then from the 17.6 MeV state.

The contaminant line marked by $^{27}$Al is coming from the $^{27}\mathrm{Al}(p,\gamma)^{28}\mathrm{Si}$ reaction induced on the backing of the target.

As the branching ratio for the decay of the 18.15 MeV state was very much unfavored, to derive the angular correlations, we set a wide gate from 13 MeV to 20 MeV, covering both the ground state transition and the transition to the first excited state. The result is shown in Fig. 3.

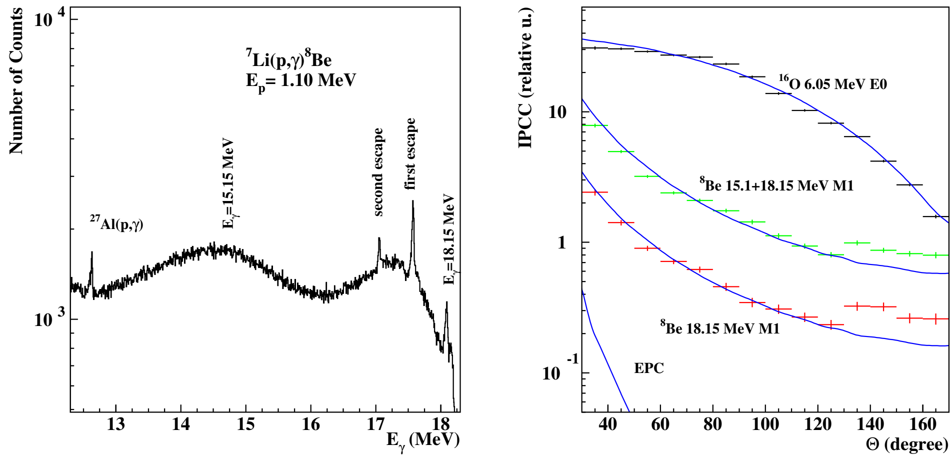


Fig. 3. (Color online) A typical $\gamma$-ray spectrum (left panel) and angular correlation of the $e^+e^-$ pairs (right panel) originated from the decay of the 18.15 MeV resonance compared with the simulated angular correlations [8] assuming M1+1.4%E1 mixed transitions (solid blue curve), measured at $E_p = 1100$ keV. The contribution of external pair creation in the simulations, caused by the 18.15 MeV $\gamma$rays is shown at the bottom of the figure marked by EPC.

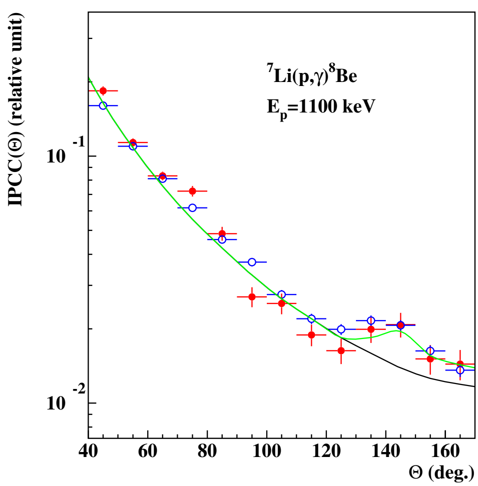


Fig. 4. (Color online) Measured angular correlations published previously [1] (blue circles) and the present results (full red dots) of the $e^+e^-$ pairs originated from the decay of the 18.15 MeV ground state transition in $^8$Be. The black line represents the background, while the gray/green one is the sum of the signal and background.

In order to check the efficiency of the experimental setup, we calculated the angular correlation also for the 6.05 MeV E0 transition coming from the $^{19}\mathrm{F}(p, \alpha\, e^+e^-)^{16}\mathrm{O}$ reaction. It is shown in the upper curve of Fig. 2 (b) together with the simulated results for an E0 transition.

Figure 4 shows our experimental results (full red dots with error bars) for the recent angular correlation of $e^+e^-$ pairs together with our previous results (open blue dots with error bars) [1] measured at the proton absorption resonance at $\mathrm{E}_p = 1030$ keV. There is very good agreement between the two independent sets of experimental data.

## 6. Fitting the measured angular correlations

The $e^+e^-$ angular correlation distribution is described by an exponentially falling distribution modeled after the IPC simulation, and the signal distribution modeled from the simulation of a boson decaying to $e^+e^-$ pairs.

The fit was performed with RooFit [10] by describing the $e^+e^-$ angular correlation distribution with the following probability density function (PDF):

$$\mathrm{PDF}(e^+e^-) = N_{\mathrm{bkgd}} * \mathrm{PDF}(\mathrm{IPC}) + N_{\mathrm{sig}} * \mathrm{PDF}(\mathrm{signal})\,, \qquad (1)$$

where $N_{\mathrm{bkgd}}$ and $N_{\mathrm{sig}}$ are the fitted number of background and signal events, respectively.

The signal PDF was constructed as a 2-dimensional model as a function of the $e^+e^-$ opening angle and the mass of the simulated particle. To construct the mass dependence, the PDF linearly interpolates the $e^+e^-$ opening angle distributions simulated for discrete particle masses.

Using the composite PDF described in Eq. (1), we first performed a list of fits, by fixing the simulated particle mass in the signal PDF to a certain value, and letting RooFit estimate the best values for $N_{\mathrm{sig}}$ and $N_{\mathrm{bkgd}}$. The best fitted values of the likelihood used to minimise the fit.

Letting the particle mass lose in the fit, the best fitted mass and the branching ratio of the $e^+e^-$ decay of such a boson to the $\gamma$ decay is calculated for the best fit. The results of the two fits are summarized in Table I.

The first column shows our published results in Ref. [1], while the second one was obtained also for the data of Ref. [1], but fitted with the method described above.

The discrepancy in the particle masses of the two data sets could be a result of the unstable beam position in our previous experiment. According to MC simulations, such a mm order of beam position variation can cause a systematic uncertainty that cannot be neglected.

TABLE I

Results of the new fit for Exp1, which was published earlier [1] and for Exp2, which is the present experiment.

| | Previous res. [1] | Exp1 | Exp2 | Average |
|---|---|---|---|---|
| $m_0c^2$ [MeV] | 16.70(51) | 16.86(6) | 17.17(7) | 17.01(16) |
| $B_x$ | $5.8\times10^{-6}$ | $6.8(10)\times10^{-6}$ | $4.7(21)\times10^{-6}$ | $6(1)\times10^{-6}$ |
| Significance | $6.8\sigma$ | $7.37\sigma$ | $4.90\sigma$ | |

The particle masses deduced from the two data sets differ more than the statistical errors. It may be caused by the uncertainty of the beam position on the target, or some misalignment of the detectors which effects the angle determination.

## 7. Results for the $^4$He transitions

We used resonant proton capture reaction on $^3$H at $E_p = 1.00$ MeV to excite the first two excited states ($J^\pi = 0^+$, and $0^-$) in $^4$He as shown in Fig. 5 (a).

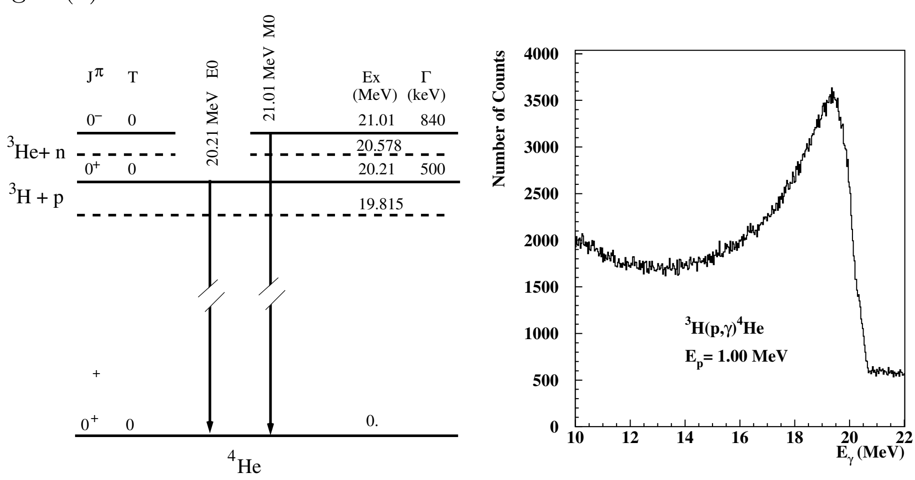


Fig. 5. The lowest energy levels of $^4$He excited in the $^3$H$(p,\gamma)^4$He reaction at a proton bombarding energy of 1.00 MeV (left panel). Measured $\gamma$-ray energy spectrum obtained from the $^3$H$(p,\gamma)^4$He direct proton capture reaction (right panel).

$\gamma$ transitions between these states and the ground state, which has a $J^\pi = 0^+$ are strictly forbidden. However, from direct proton capture, we were expecting $\gamma$ rays as well, to the ground state of $^4$He, as shown in Fig. 5 (b). Such energetic $\gamma$ rays create $e^+e^-$ pairs in the Mo backing of the target, as well as in other materials surrounding the target by external pair creation.

The two excited states in $^4$He are strongly overlapping. With an $E_p =$ 1.000 MeV bombarding energy, the excitation energy is 20.6 MeV, which is in between the two excited states, so both states are excited. We are expecting $e^+e^-$ pairs from the E0 transition of $0^+ \to 0^+$, but no pairs from $0^- \to 0^+$. transition. However, if an $X(17)$ particle is created, then from its decay one can expect $e^+e^-$ pairs with well-defined correlation angles.

The experimental $e^+e^-$ angular correlation is shown in Fig. 6 (a) by full red dots with error bars. The solid curves with different colors are the result of our Monte-Carlo (GEANT4) simulations. The angular correlation is dominated by the $e^+e^-$ pairs expected from the $0^+ \to 0^+$ E0 transition (gray/purple). It has another important contribution from the external pair creation (EPC) of the $\gamma$ rays (black). We can observe also a small anomaly at about $\Theta = 115°$, which corresponds to the $e^+e^-$ decay of the $X(17)$ particle (light gray/green).

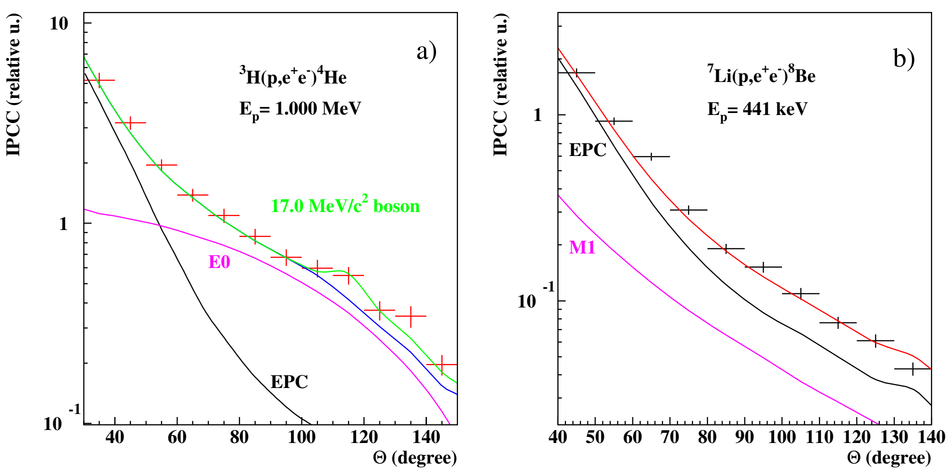


Fig. 6. (Color online) Measured angular correlations of the $e^+e^-$ pairs originated from the decay of the 20.6 MeV transition excited in the $^3$H$(p,\gamma)^4$He reaction (a) and from the 17.6 MeV ground state transition in $^8$Be (b)

In order to calibrate the spectrometer and check the effect of the Mo backing, we performed experiments using the well-known $^7$Li$(p,\gamma)^8$Be reaction having no Mo backing and having 0.4 mm thick Mo backing. Without a Mo backing, the angular correlation could nicely be reproduced with the simulated curve obtained for M1 internal pair creation. The angular correlation measured with Mo backing is shown in Fig. 6 (b). It is dominated by external pair creation (EPC). The internal pair creation of the 17.6 MeV M1 transition has only a small contribution to this angular correlation.

## 8. Conclusions

We have remeasured the $e^+e^-$ angular correlation for the M1 transition depopulating the 18.15 MeV state in $^8$Be. We could reproduce the peak-like deviation from the predicted IPC, confirming the signal of the new $X(17)$ particle as well as constraining its mass ($m_0c^2 = 17.01(16)$ MeV) and branching ratio compared to the $\gamma$ decay ($B_x = 6(1) \times 10^{-6}$). We have measured the $e^+e^-$ angular correlation for the mixture of the high-energy (20.6 MeV) $J^\pi = 0^- \to 0^+$ and $J^\pi = 0^+ \to 0^+$ transitions in $^4$He as well. Although the second transition (E0) gave a large background, the effect of the $X(17)$ $e^+e^-$ decay was also visible at 115 degree. We are planning to repeat the experiment with better statistics. Using better energy resolution and a sharper cut on the symmetry energy will also help to improve the signal/background ratio.

This work was supported by the National Research, Development and Innovation Fund of Hungary, financed under the K17 funding scheme with project No. K124810, by the GINOP-2.3.3-15-2016-00034 and by the János Bolyai Research Fellowship of the Hungarian Academy of Sciences (L. Csige).

REFERENCES

[1] A.J. Krasznahorkay *et al.*, *Phys. Rev. Lett.* **116**, 042501 (2016).

[2] `https://inspirehep.net/search?ln=en&p=refersto%3Arecid%3A1358248&jrec=26&sf=earliestdate`

[3] X. Zhang, G.A. Miller, *Phys. Lett. B* **773**, 159 (2017).

[4] J. Feng *et al.*, *Phys. Rev. Lett.* **117**, 071803 (2016).

[5] J. Feng *et al.*, *Phys. Rev. D* **95**, 035017 (2017).

[6] U. Ellwanger, S. Moretti, *J. High Energy Phys.* **1611**, 039 (2016).

[7] D.R. Tilley *et al.*, *Nucl. Phys. A* **745**, 155 (2004).

[8] J. Gulyás *et al.*, *Nucl. Instrum. Methods Phys. Res. A* **808**, 21 (2016).

[9] R. Tilley, H.R. Weller, G.M. Hale, *Nucl. Phys. A* **541**, 1 (1992).

[10] W. Verkerke, D.P. Kirkby, *The RooFit Toolkit for Data Modeling*, *eConf C* **0303241** (2003) MOLT007 [arXiv:physics/0306116 [physics.data-an]].